Available online at www.CivileJournal.org

Civil Engineering Journal

(E-ISSN: 2476-3055; ISSN: 2676-6957)

Vol. 9, No. 07, July, 2023

Four-Face Heated Uniaxial Reinforced Concrete Columns Interaction Charts

Mohammed S. Al-Ansari [1*], Muhammad S. Afzal [2]

[1] *Professor, Department of Civil and Architectural Engineering, Qatar University, Doha, Qatar.*

[2] *Graduate Student, Department of Civil, Architectural and Environmental Engineering, University of Texas at Austin, USA.*

Received 27 December 2022; Revised 07 June 2023; Accepted 19 June 2023; Published 01 July 2023

Abstract

This paper presents an analytical method for generating the interaction diagrams of uniaxially reinforced concrete (RC) columns that are subjected to four-face heating. Twenty-one (21) specimens obtained from previous case studies that were subjected to four-face heating (with different fire test times ranging from 63 to 356 fire minutes) are used to validate the proposed uniaxial interaction charts. The results obtained from the case studies and from the proposed charts are also compared with the finite element software (FIN EC). The 500°C isotherm as well as the zone method are used in the computer software program to find the required load capacities. The proposed method's values fall within the range of values obtained from laboratory tests and computer software, which suggests its validity. Also, the zone method in FIN-EC software is reliable for evaluating load-bearing capacity, while the 500°C method is useful in situations with shorter fire times. The results obtained provide a valuable tool for designing and evaluating structures that may be exposed to fire. Nonetheless, the study is restricted by its concentration on a particular type of column under four-face heating, which may reduce its relevance to other types of structures and heating situations.

Keywords: Uniaxial Columns; 4-Face Heating; Fire Time; Interaction Charts; Axial Load Capacity.

1. Introduction

In the construction industry, reinforced concrete (RC) columns are widely used as load-bearing components in buildings due to their durability, strength, and cost-effectiveness. However, they are vulnerable to fire, which can significantly reduce their load-bearing capacity and cause structural collapse [1–3]. Investigating the fire resistance of RC structures, particularly columns, is crucial for building stability. Columns are vertical members that transfer loads from upper floors to lower levels and to the soil through the foundation. They are classified as concentrically or eccentrically loaded based on the load position on their cross-section, as shown in Figures 1 and 2 [4]. Reinforced concrete (RC) columns are prone to significant reductions in their load-bearing capacity when subjected to higher temperatures caused by fire. This is due to the degradation of strength and stiffness in both concrete and steel materials. However, predicting the fire resistance of RC columns is challenging due to the complex distribution of temperatures in the column's cross-section, resulting in a shortage of simplified and rational methods for predicting fire resistance [5].

Numerous studies have focused on experimental methods for investigating the fire resistance of reinforced concrete columns, and their experimental results revealed that several factors, such as the concrete cover, the reinforcement's size and location, and the type and duration of the fire exposure, significantly affect the fire resistance of reinforced concrete

* Corresponding author: m.alansari@qu.edu.qa

http://dx.doi.org/10.28991/CEJ-2023-09-07-01

columns. However, the cost and time involved in conducting such tests are often prohibitively high, making it challenging to conduct a sufficient number of tests to develop a comprehensive understanding of the behavior of reinforced concrete columns under fire conditions [6–13].

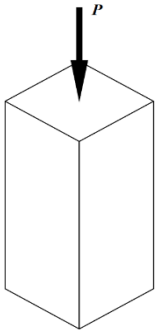

Figure 1. Concentrically Loaded columns

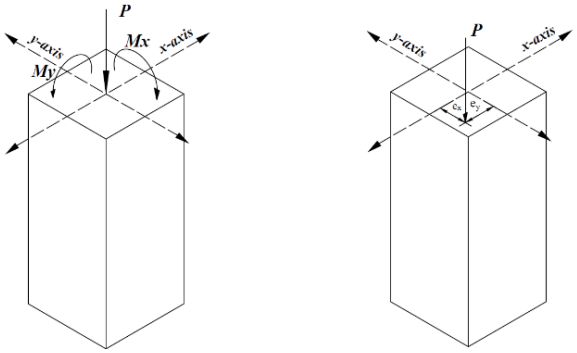

Figure 2. Eccentrically Loaded Column

Current concrete structure design standards are mostly based on national and international code guidelines, such as ENV 1992-1-2 (European Council for Standardization, 1995) [14]. In order to construct fire-exposed concrete columns, these codes give tabular data with the requisite concrete cover for various fire durations. Nevertheless, this process should be augmented with engineering theory-based easy computation methods [15]. Concrete material characteristics under fire circumstances have been studied, and simpler techniques for estimating the fire resistance of RC columns have been devised [1-3, 16-18]. Due to the complicated temperature distribution in the cross-section of RC columns and the significant dispersion of experimental data generated by spalling of the concrete [19, 20], the application of simple and logical approaches for predicting fire resistance in RC columns is still restricted.

Analytical calculations offer a faster and cheaper alternative to traditional experiments. Developing quick and efficient methods for the design prediction of concrete columns under fire conditions is essential, particularly as simulating concrete members' behavior during a fire is difficult, and consulting engineers may not have access to the necessary numerical tools [17]. The latest knowledge gap is the need for more efficient and quick analytical formulations for predicting fire resistance in RC columns to withstand fires.

This study presents a method for generating interaction diagrams of uniaxial reinforced concrete (RC) columns exposed to four-face heating. These interaction diagrams presented, account for the various values of gamma (γ), concrete compressive strength (f_c'), and steel reinforcement ratio (ρ). Using interaction charts, numerical examples will also be analyzed to determine the values of (P_N) and (M_N). These formulated uniaxial interaction charts are validated using twenty-one (21) specimens obtained from previous case studies [7, 8, 17] and subjected to four face heating *(having different fire testing time ranging from 63 to 356 fire minutes*). Furthermore, the results obtained from the case studies are compared to those obtained from the finite element simulation software (FIN EC) [21]. In the computer program, the 500°C isotherm and zone method are used to calculate the required axial load capacities of RC columns subjected to four-faced heating.

Interaction diagrams are commonly used to represent the strength of reinforced concrete columns by relating the design axial load $\emptyset P_n$ to the design bending moment $\emptyset M_n$. Figure 3 [18] shows the column interaction curve $(\emptyset P_n - \emptyset M_n)$ at ambient temperature and when exposed to a shorter and longer duration of fire. With an increase in temperature, the force-moment interaction diagram (P-M) contracts. A heating curve, such as ISO 834 [22] can be used to determine the relationship between temperature *(T)* and fire exposure time *(t)*. By comparing the initial applied load with the failure load at a given fire exposure time, it is possible to ascertain the occurrence of column failure.

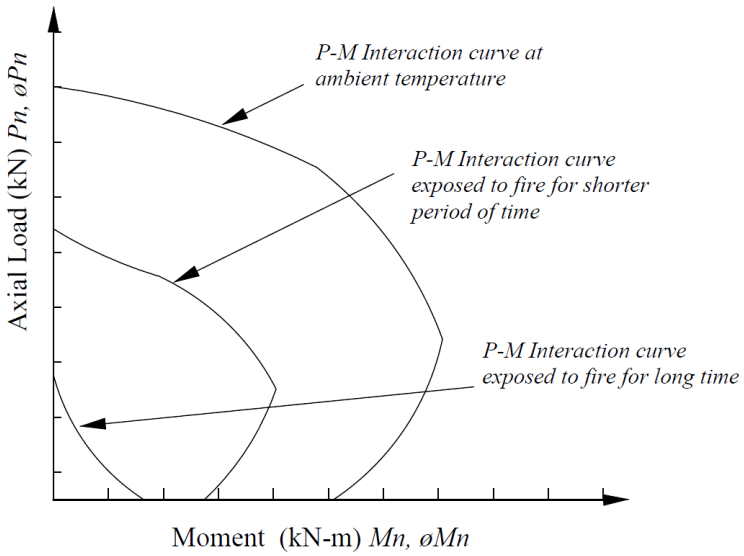

Figure 3. ($\emptyset P_n - \emptyset M_n$) Interaction curve exposed to elevated temperature [18]

According to the structural architecture depicted in Figure 4 [19], a building's columns may be vulnerable to fire on one, two, three, or all four sides. While estimating the fire resistance of RC columns, it is essential to evaluate the deterioration of concrete and steel properties, as well as the movement of the neutral axis. In this study, the authors are only considering the middle columns of the building, which are normally subjected to four-face heating. To determine the approximate column capacity (4-face heated) under different fire exposure times, the proposed method will develop interaction charts in SI (system international) units for any internal column of the building.

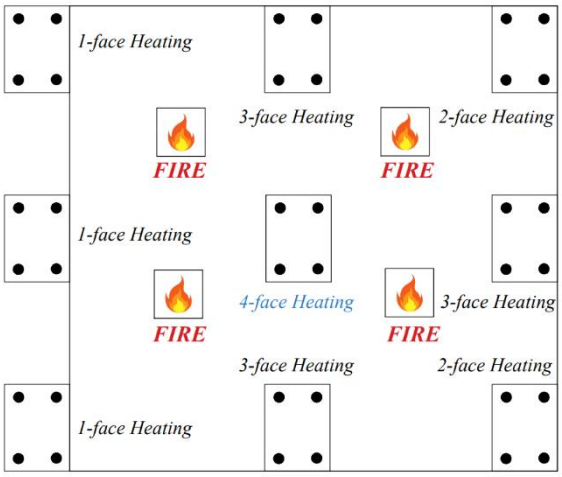

Figure 4. Columns in a compartment with different thermal boundary conditions [19]

2. Fire Reduction Factors

The fire reduction factors used in this research are obtained from a study done by Tan & Yao [5]. In the event of a fire breaking out in a reinforced concrete (RC) building, there is a significant reduction in the strength of concrete and steel rebars. Thus, the reduction factors in calculating the respective strengths serve as critical components when determining the new design strengths of RC columns. Dotreppe et al. [7] conducted a thermal analysis and employed the SAFIR [23] computer code to evaluate the behavior of RC columns subjected to ISO 834 fire. As a result, they determined that the expressions, ϕ_{c-4} and ϕ_{y-4}, are suitable to represent the strength reduction factors for concrete and corner steel bars, respectively, when the columns are exposed to four-face heating.

The reduction factor for the concrete having four face heating (ϕ_{c-4}) is provided in Equation 1:

$$\phi_{c-4} = \frac{\gamma(t_{(ISO)})}{\sqrt{1+(0.3A_c^{-0.5}t_{ISO})A_c^{-0.25}}} \quad (1)$$

where, $t_{(ISO)}$ = ISO 834 fire exposure time in hours; A_c= cross-sectional area in m^2; f_c' = concrete cylinder strength (MPa) at ambient temperature. The reduced compressive strength of concrete (f_{cT}') will be:

$$f'_{cT} = \phi_{c-4} \times f'_c \quad (2)$$

Equation 3 provides the reduction factor for steel bar (ϕ_{y-4}) subjected to four-face heating.

$$\phi_{y-4} = \gamma(t_{(ISO)}) \left(1 - \frac{0.9t_{(ISO)}}{0.046d' + 0.11}\right) \geq 0 \quad (3)$$

where, $d'$is concrete cover in mm (from edge fiber to center of the steel bar), and $\gamma(t_{(ISO)}) = \begin{cases} 1 - 0.3t_{(ISO)} & for\ t \geq 0.5\ h \\ 0.85 & for\ t < 0.5\ h \end{cases}$

Similarly, the reduced computed steel stress (f_{yT}) in tensile steel will be:

$$f_{yT} = \phi_{y-4} \times f_y \quad (4)$$

Equations 1 to 4 are only applicable to RC columns satisfying the following conditions:

- Siliceous aggregates
- Subjected to ISO 834 fire
- For rectangular section with $b/h < 2.0$, where b and h are the width and depth of the column cross section.

Tan & Yao [5] also proposed the reduction factor $\phi_{ES}(t)$ for the steel elastic modulus $E_s(T)$ as provided in Equation 5.

$$\phi_{ES}(t) = 0.8 \times (\phi_{y-4})^2 + 0.2 \times \phi_{y-4} \quad (5)$$

The reduction factor for the steel elastic modulus, denoted as $\phi_{ES}(t)$, depends on three factors: the concrete cover, the temperature distribution across the cross-section, and the fire curve. Figure 5 illustrates the relationship between the reduction factor of the steel elastic modulus ($\phi_{ES}(t)$) and the duration of fire exposure *(t)* for four distinct concrete covers. The chart data is obtained from Tan & Yao [5]. It shows that the reduction factor is almost zero after 2.5 hours of fire time.

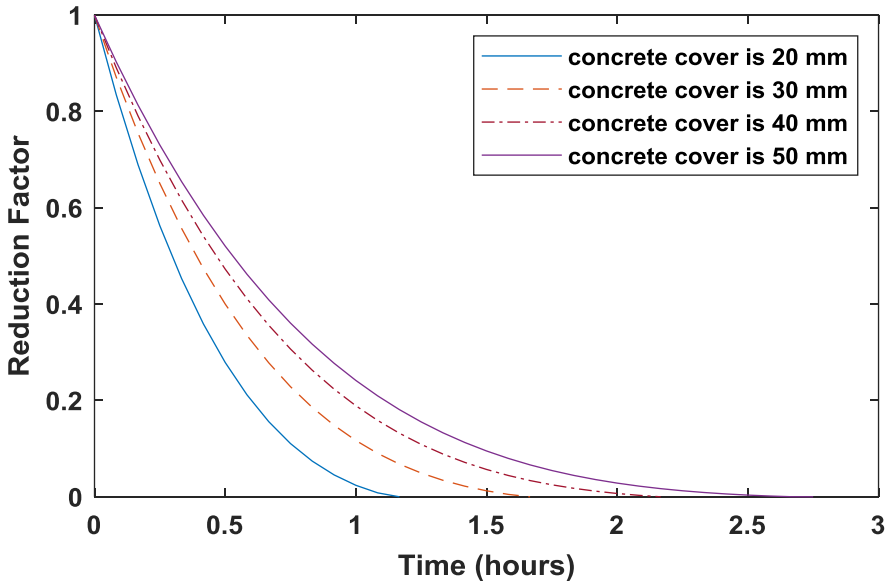

Figure 5. Relationship between reduction factor $\phi_{ES}(t)$ and fire exposure time *(t)* corresponding to different concrete covers [5]

For the concrete, Tan & Yao [5] have also provided a method to derive the reduction factor $\phi_{EcI}(t)$ for the modulus of elasticity of concrete, $E_C(T)$. In their study, they indicated that due to the nonlinear distribution of temperature, unlike steel, deterioration factor should be related to all cross-sectional elements. They combined the modulus of Elasticity E with the moment of Inertia I to have the E_CI value with the reason of rapid deterioration of strength and modulus of elasticity of outer fiber of cross section under a fire attack on column. They proposed the following Equation 6 for the concrete elastic modulus reduction factor.

$$\phi_{EcI}(t) = (1.1 \times A_C^{0.15})^{t_{ISO}} \times \phi_{C-4}(t) \quad (6)$$

The equation presented above is derived from the correlation between the reduction factor $\phi_{EcI}(t)$ and the duration

of fire exposure *(t)* for four distinct square cross sections, as illustrated in Figure 6. This chart is also extracted from Tan & Yao [5].

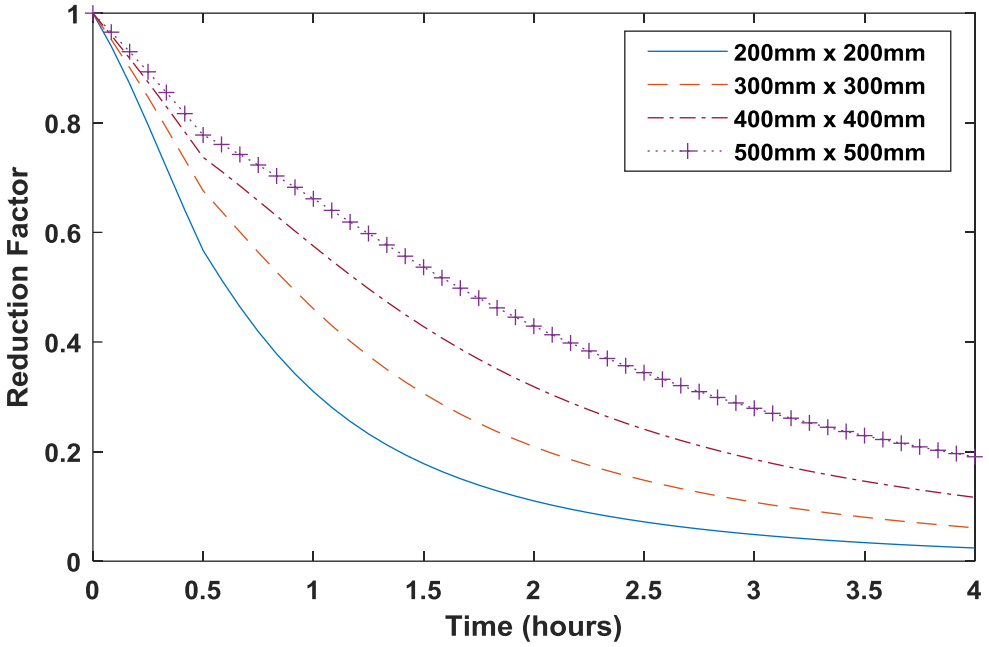

Figure 6. Relationship between reduction factor $\phi_{EcI}(t)$ and fire exposure time *(t)* corresponding to different cross sections [5]

Moreover, they also proposed a set of values for strain failure criterion $\varepsilon_U(T)$ corresponding to different temperatures as provided in Table -1. Strain can be interpolated between any two temperatures using linear interpolation. They have also mentioned that the values provided in table -1 are obtained from the addition of 0.5 x 10^{-3} strain to the corresponding yield strain $\varepsilon(T)$ in EC2-1992-1-2 [14]. Additionally, if experimental data for $\varepsilon_U(T)$ is available, Table 1 can be updated accordingly.

Table 1. Value of $\varepsilon_U(T)$ [18]

Concrete Temperature (^{0}C)	20	100	200	300	400	500	600	700	800	900	1000
t_{ISO} (min)	0	0.16	0.29	0.69	1.45	2.95	5.87	11.6	22.7	44.3	86.5
$\varepsilon_U(T) \times 10^{-3}$	3.0	4.0	5.0	6.5	8.0	10.0	13.0	14.5	15.0	15.5	15.5

According to the ACI Code [21] for design under ambient temperatures, the depth of the rectangular stress block a_b can be represented by the following equation:

$$a_b = \beta_1 c_b \tag{7}$$

The strain in the compression steel $\varepsilon_s'(T)$ is obtained from below Equation 8.

$$\varepsilon_s'(T) = \varepsilon_U(T)\frac{c_b - d'}{c_b} \tag{8}$$

where, c_b is the neutral axis depth and $d'$is concrete cover in mm *(from edge fiber to centre of the steel bar)*. The $\varepsilon_U(T)$ value needs to be obtained from Table 1.

3. Derivation of Interaction Charts Formulation using ACI Code of Design

In previous studies, Al-Ansari & Afzal [4, 24], the authors have presented analytical methods for generating interaction diagrams in SI units for the design of reinforced concrete (RC) uniaxial and biaxial columns [25]. The ACI code [26] is used to generate interaction diagrams for uniaxial reinforced concrete (RC) columns under four-faced heating, and the process involved the following steps. Figure 7 [27] provides the stress and strain distribution of a rectangular column section (at elevated temperature) subjected to fire, which was used to calculate P_N and M_N for the diagram.

The total internal forces can be added together to obtain the resulting force P_N ($P_N = C_C - T_s + C_S$). Likewise, the total internal moments can be added together to obtain the resulting moment M_N ($M_N = M_{conc} + M_T + M_{C_S}$). The subsequent steps involved computing the necessary internal forces and moments.

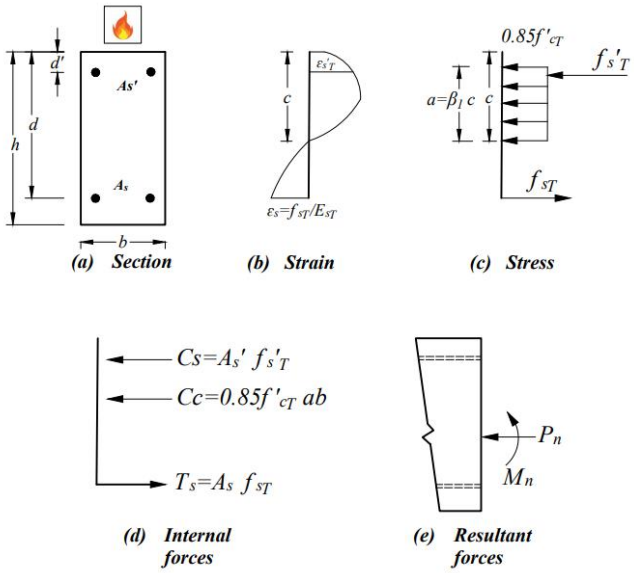

Figure 7. Calculation of P_N and M_N for given strain distribution at elevated temperature [27]

3.1. Concrete Section

$$C_{conc} = 0.8 \times (0.85\, f'_{cT}\, ab) = 0.68\, f'_{cT}\, \beta_1 cb \tag{9}$$

where C_{conc} is internal concrete compression force, f'_{cT} is reduced compressive concrete strength *(obtaining from Eq-2)*, b is Column width, a is depth of the compression stress block, $\beta_1 = 0.85 - 0.05 \times \left(\frac{f'_c(T)}{6.9} - 4\right) \geq 0.65$ *(retrieved from* Tan & Yao [5]), c is distance from extreme compression fiber to neutral axis.

Referring to the Figure 7, the moment about the midpoint of the section (M_{conc}) can be computed as;

$$M_{conc} = 0.68\, f'_{cT}\, ab \left(\frac{h}{2} - \frac{a}{2}\right) \tag{10}$$

The α_1 and β_1 values for the plain concrete section are calculated as;

$$Setting\ \alpha_{1-conc} = \alpha_1 = \frac{C_{conc}}{f'_{cT}\, bh} = 0.68 \times \frac{a}{h} \tag{11}$$

$$Setting\ \beta_{1-conc} = \beta_1 = \frac{M_{conc}}{f'_{cT}\, bh^2} = 0.68 \left(\frac{h}{2} - \frac{a}{2}\right) \times \frac{1}{h} \times \frac{a}{h} \tag{12}$$

3.2. Tension Steel Section

The calculation for the internal tensile force *(T_s)* is as follows:

$$T_s = 0.68\, A_s f_{yT} \tag{13}$$

where A_s is area of tensile steel reinforcement, and f_{yT} is reduced computed steel stress in tensile steel.

The value of the internal moment M_T is;

$$M_T = 0.68\, A_s f_{yT} \left(\frac{h}{2} - d'\right) \tag{14}$$

The values of α_2 and β_2 for the tension steel section can be computed using the following equations:

$$Setting\ \alpha_2 = \frac{T_s}{f'_{cT}\, bh} = \frac{0.68\, A_s f_{yT}}{f'_{cT}\, bh} = \rho_2 \frac{0.68 f_{yT}}{f'_{cT}} \tag{15}$$

$$Setting\ \beta_2 = \frac{M_T}{f'_{cT}\, bh^2} = 0.68 \frac{A_s f_{yT}\left(\frac{h}{2} - d'\right)}{f'_{cT}\, bh^2} \tag{16}$$

Substituting the value of α_2 in the Equation16;

$$\beta_2 = \left(\frac{1}{2} - \frac{d'}{h}\right)\alpha_2 \quad (17)$$

where d' is Distance from extreme compression fibre to centroid of reinforcing steel.

3.3. Compression Steel Section

The calculation for the internal compressive force (Cs) is as follows:

$$C_s = 0.8\, A_s' f'_{sT} \quad (18)$$

where $A_s{}'$ is area of compression steel reinforcement, and f'_{sT} is reduced computed compressive stress in compression steel. The value of the internal moment M_{CS} is;

$$M_{CS} = 0.8\, A_s{}' f'_{sT} \left(\frac{h}{2} - d'\right) \quad (19)$$

The values of α_3 and β_3 for the compression steel section can be computed using the following equations:

$$Setting\ \alpha_3 = \frac{C_s}{f_{cT}' bh} = \frac{0.8\, A_s{}' f'_{sT}}{f_{cT}' b\, h} = \frac{0.8\, A_s{}'}{b\, h} \times \frac{f'_{sT}}{f_{cT}'} = \rho_3 \frac{0.8\, f'_{sT}}{f_{cT}'} \quad (20)$$

$$Setting\ \beta_3 = \frac{M_{Cs}}{f_{cT}'\, bh^2} = 0.8\, \frac{A_s{}' f'_{sT} \left(\frac{h}{2} - d'\right)}{f_{cT}'\, bh^2} \quad (21)$$

Substituting the value of α_3 in Equation 21;

$$\beta_3 = \left(\frac{1}{2} - \frac{d'}{h}\right)\alpha_3 \quad (22)$$

4. Construction of Interaction Chart

The total axial load capacity of column is summation of all internal forces P_N where;

$$P_N = C_{Con} - T + C_S \quad (23)$$

Therefore, $\alpha = \alpha_1 - \alpha_2 + \alpha_3$

$$\alpha = 0.68 \times \frac{a}{h} - \rho_2 \frac{0.68\, f_{yT}}{f_{cT}'} + \rho_3 \frac{0.8\, f'_{sT}}{f_{cT}'} \quad (24)$$

$$P_N = \alpha\, b\, h \quad (25)$$

For the nominal moment capacity, the column nominal moment M_N is summation of all internal moments *where*

$$M_N = M_{Con} + M_T + M_{C_S} \quad (26)$$

Therefore $\beta = \beta_1 + \beta_2 + \beta_3$

$$\beta = 0.68 \left(\frac{h}{2} - \frac{a}{2}\right) \times \frac{1}{h} \times \frac{a}{h} + \left(\frac{1}{2} - \frac{d'}{h}\right)\alpha_2 + \left(\frac{1}{2} - \frac{d'}{h}\right)\alpha_3 \quad (27)$$

$$M_N = \beta b\, h^2 \quad (28)$$

The Equations 25 and 28 are used to calculate the values of α ($\alpha = \frac{P_N}{bh} = \frac{P_N}{A_g}$) and β ($\beta = \frac{M_N}{bh^2} = \frac{M_N}{A_g h}$).

To determine the value of Gamma (γ) for the column interaction chart, the following calculation is performed:

$$\gamma = \frac{h - 2\, d'}{h} \quad (29)$$

Table 2 displays the values of $\left(\frac{d'}{h}\right)$ corresponding to various values of γ, which will be utilized in Equation 19.

Table 2. Values of γ vs (d'/h)

Sr. No	γ	$\frac{d'}{h}$
1	0.6	0.2
2	0.7	0.15
3	0.8	0.1
4	0.9	0.05

Thus, by successfully assigning different values to $\left(\frac{a}{h}\right)$ and substituting in Equations 24 and 27, the column interaction diagram curve $(\beta - \alpha)$ can be constructed. Using the above steps, the interaction charts for RC column having different reinforcement ratios (ρ) with f_c' = 30 MPa; fy = 415 MPa; γ= 0.6 without any fire outbreak *(t=0 minute)* and with the fire of 70 minutes time are provided in Figures 8 and 9 respectively. The flow chart for generating interaction charts is provided in Figure 10.

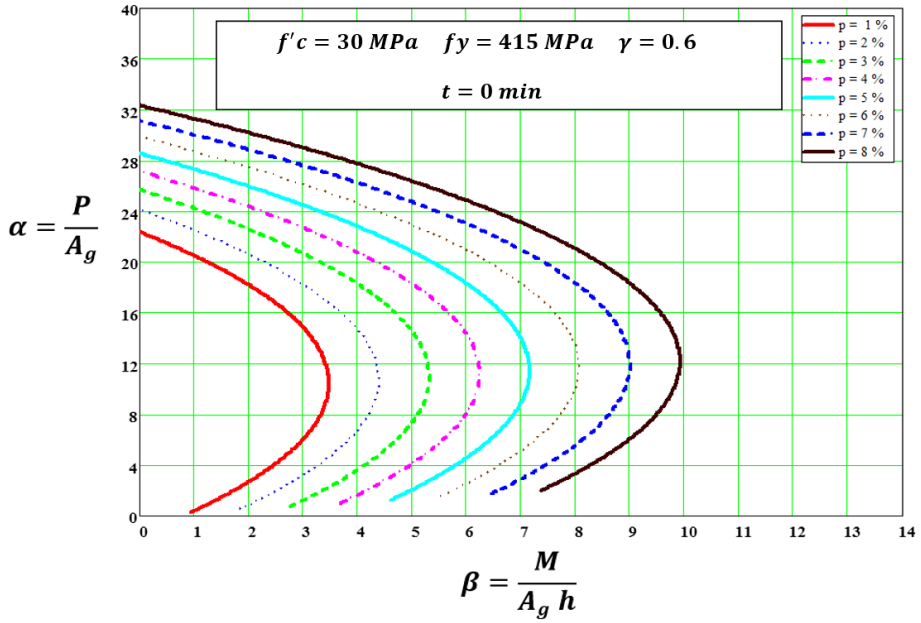

Figure 8. Column Interaction Diagram ($\beta - \alpha$) without fire

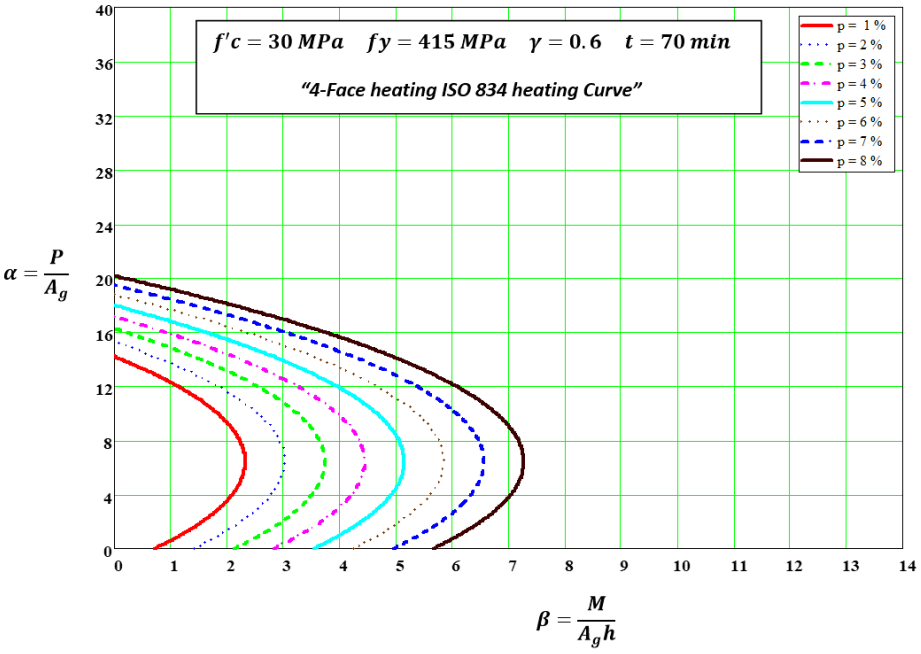

Figure 9. Column Interaction Diagram *(β- α)* with fire time, t= 70 minutes

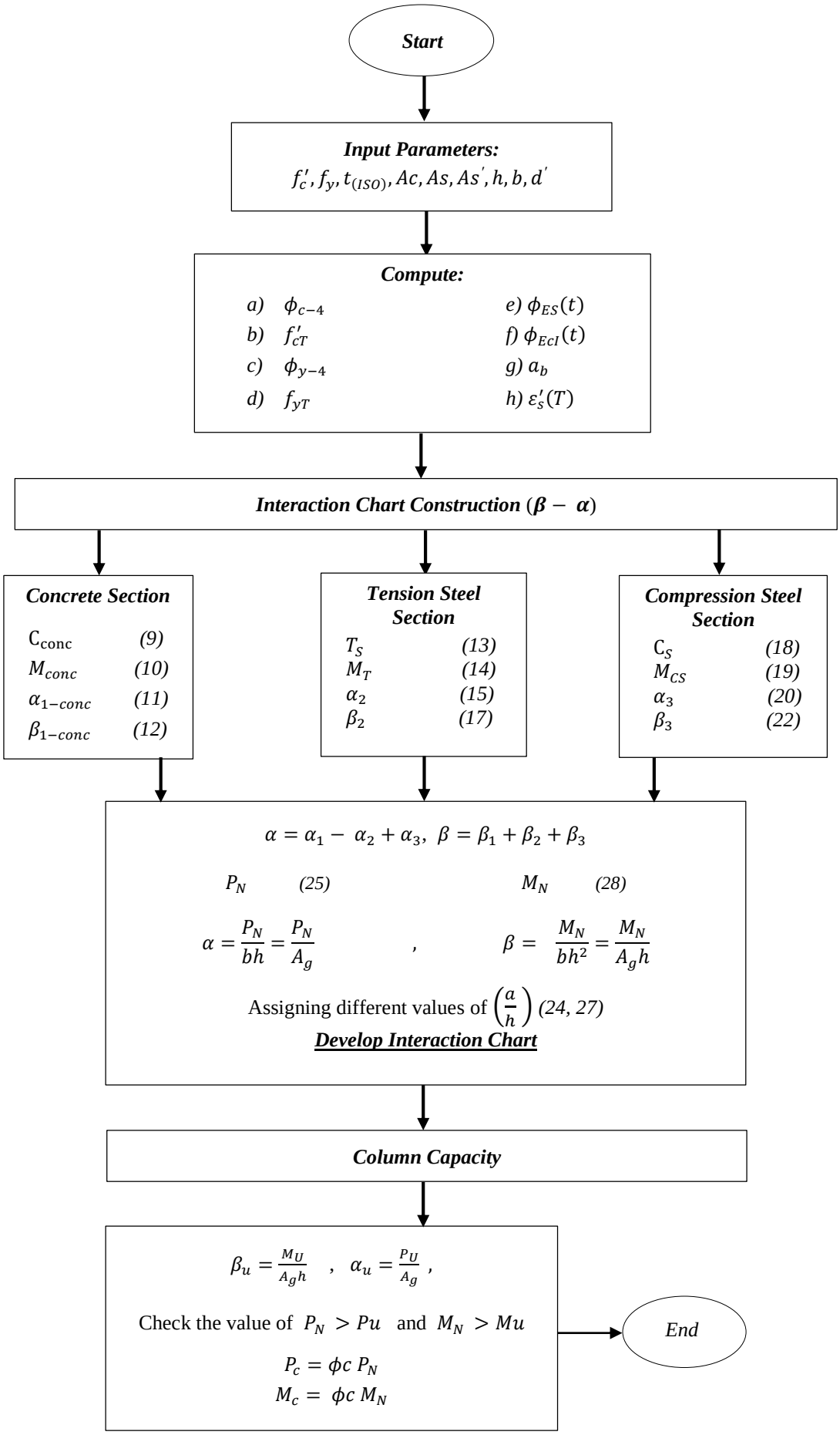

Figure 10. Flow chart of generating Interaction Charts

4.1. Steps to find the P_N and M_N

To achieve an economical design, the subsequent steps must be carried out to calculate the values of Pc and Mc.

Step-1: Determine f'_{cT} and f_{yT} from Equations 2 and 4.

Step-2: Determine the value of β_u ($\beta_u = \frac{M_U}{A_g h}$) using the provided cross-section and moments (Mu).

Step-3: Calculate the value of α_u ($\alpha_u = \frac{P_U}{A_g}$) using the given cross-section and axial load (Pu)

Step-4: Draw a line from the origin (0,0) through point (β_u , α_u) to the specified ρ line.

Step-5: Identify the new points (β, α) located on the desired ρ line, as illustrated in Figure 11.

Step-6: Compute $P_N = \alpha b\, h$ and $M_N = \beta b\, h^2$.

Step-7: To ensure an acceptable design with $\phi_c = 1$, verify that the value of P_N is greater than Pu and that M_N is greater than Mu.

Step-8: To achieve an economical section, the values of $Mc = \phi_c M_N$ and $Pc = \phi_c P_N$ should be as close as possible to Mu and Pu, respectively, where ϕ_c is equal to 0.65.

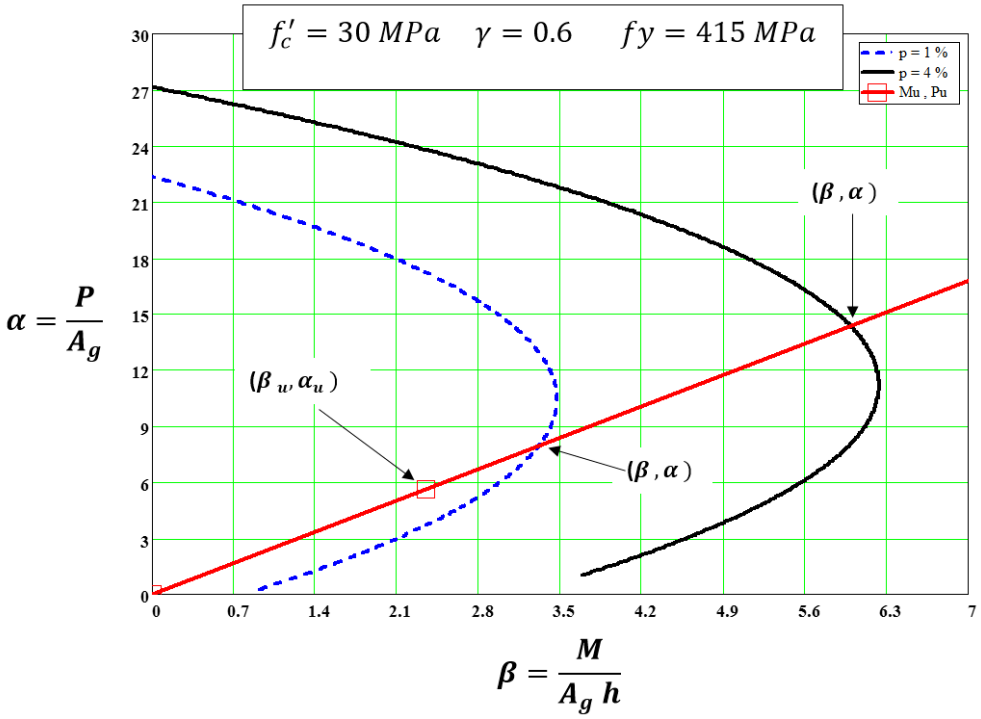

Figure 11. Column Interaction Diagram ($\beta - \alpha$) Demonstration

5. Case Studies for Uniaxial Bending

The proposed interaction charts are used to predict the fire resistance of square and rectangular RC columns. Twenty-one data sets of RC columns from two different laboratories (Lie & Woollerton [8] and Dotreppe, et al., [7]) were retrieved from the literature and the results were compared with the proposed method. All these selected columns were subjected to four face hearing. Wu, et al., [17] also presented an approach for calculating the axial load of square cross-section RC columns. Their study was performed on some of the selected square columns provided by Lie & Woollerton [8].

In this study, input data and results obtained from three case studies will be used. The data for the case study -1 and 2 are obtained from (Lie & Woollerton [8]) and (Wu et al. [17]). Sixteen columns (Column C-1 to C-16) were selected from these case studies. The input parameters as well as the axial load capacity of these selected RC columns for case studies 1 and 2 are listed in Table 3. In the case study of (Wu et al. [17]) there were no output results for columns C-12 to C-16 and therefore written NA in axial load section. The details of case study -3 (Dotreppe, et al. [7]) are depicted in Table 4. Five columns (Column C-17 to C-21) are included in this case study. For each case study, the RC column is similar in length. The length of the column for case studies 1 and 2 is 3.81 m, and the length of the column for case study 3 is 2.1 m.

Table 3. Details of Case Study 1 and 2 (Lie & Woollerton [8]) and (Wu et al. [17])

Column Identifier	Reference*	*b* (mm)	*h* (mm)	Rebar (mm)	End[c]	*fy* (MPa)	f'_c (MPa)	t_{test} (min)	Axial Load[a] (kN)	Axial Load[b] (kN)
C-1	I2	305	305	4 Ø25.5	f-f	444	36.9	170	1333	517.2
C-2	I3	305	305	4 Ø25.5	f-f	444	34.2	218	800	200
C-3	I4	305	305	4 Ø25.5	f-f	444	35.1	220	711	155
C-4	I7	305	305	4 Ø25.5	f-f	444	36.1	208	1067	339
C-5	I9	305	305	4 Ø25.5	f-f	444	38.3	187	1333	498.5
C-6	II2	305	305	4 Ø25.5	f-f	444	43.6	201	1044	268
C-7	II3	305	305	4 Ø25.5	f-f	444	35.4	210	916	255
C-8	II4	305	305	4 Ø25.5	f-f	444	52.9	227	1178	280
C-9	II5	305	305	4 Ø25.5	f-f	444	49.5	234	1067	247.5
C-10	II8	305	305	8 Ø25.5	f-f	444	42.6	252	978	242
C-11	II10	406	406	8 Ø25.5	f-f	444	38.8	262	2418	914
C-12	II12	406	406	8 Ø32.3	f-f	414	46.2	213	2978	NA
C-13	III1	305	305	4 Ø25.5	p-f	444	39.6	242	800	NA
C-14	III2	305	305	4 Ø25.5	p-f	444	39.2	220	1000	NA
C-15	III3	305	305	4 Ø25.5	p-p	444	39.9	181	1000	NA
C-16	III14	305	305	4 Ø25.5	p-f	444	37.9	183	1178	NA

[a] The axial load result values are obtained from the case study of (Lie & Woollerton, [8]).; [b] The axial load result values are obtained from the case study of (Wu, et al.,[17]).; [c] The symbol "p" stands for pinned end condition and "f" stands for fixed end condition.; * The reference columns are taken from (Lie & Woollerton, [8]).

Table 4. Details of Case Study 3 (Dotreppe et al. [7])

Column Identifier	Reference*	*b* (mm)	*h* (mm)	Rebar (mm)	End	*fy* (MPa)	f'_c (MPa)	t_{test} (min)	Axial Load (kN)
C-17	31BC	300	300	4 Ø16	p-p	576	29.3	63	1270
C-18	31CC	300	300	4 Ø16	p-p	576	28.6	123	803
C-19	33AC	300	300	4 Ø25	p-p	591	26.2	69	878
C-20	21BC	200	300	6 Ø12	p-p	493	30.6	107	611
C-21	22BC	200	300	6 Ø12	p-p	493	27.3	97	620

* The reference columns are taken from (Dotreppe, et al. [7])

The reduction factors ϕ_{c-4} and ϕ_{y-4} are calculated based on Equations 1 and 3 in order to find the reduced compressive strength, f'_{cT} and reduced steel stress, f_{yT} (Equations 2 and 4). The reduced strength values for all studied columns are provided in Tables 5 and 6 respectively.

Table 5. Reduction Factors ϕ_{c-4} and ϕ_{y-4} for case study-1 and 2

Column Identifier	t_{test} (min)	f_y (MPa)	ϕ_{y-4}[a]	f_{yT} (MPa)	f'_c (MPa)	ϕ_{c-4}	f'_{cT} (MPa)
C-1	170	444	0	0	36.9	0.313	11.532
C-2	218	444	0	0	34.2	0.256	8.751
C-3	220	444	0	0	35.1	0.254	8.914
C-4	208	444	0	0	36.1	0.266	9.599
C-5	187	444	0	0	38.3	0.29	11.1
C-6	201	444	0	0	43.6	0.273	11.922
C-7	210	444	0	0	35.4	0.264	9.34
C-8	227	444	0	0	52.9	0.247	13.091
C-9	234	444	0	0	49.5	0.241	11.944
C-10	252	444	0	0	42.6	0.227	9.661
C-11	262	444	0	0	38.8	0.219	8.515
C-12	213	414	0	0	46.2	0.361	16.68
C-13	242	444	0	0	39.6	0.235	9.291
C-14	220	444	0	0	39.2	0.254	9.955
C-15	181	444	0	0	39.9	0.297	11.868
C-16	183	444	0	0	37.9	0.295	11.175

[a] The reduction factor values for steel bars (ϕ_{y-4}) is zero as the fire time is more than 2.5 hours (150 minutes). With such higher fire time (i.e. approx. more than 2.5 hours of fire), the ϕ_{y-4} value will be negative and it should be taken as zero. In other words, after two hours of fire, the steel will be melted and its reduced yield strength will be taken as zero (MPa).

Table 6. Reduction Factors ϕ_{c-4} and ϕ_{y-4} for case study-3

Column Identifier	t_{test} (min)	f_y (MPa)	ϕ_{y-4}	f_{yT} (MPa)	f'_c (MPa)	ϕ_{c-4}	f'_{cT} (MPa)
C-17	63	576	0.213	122.4	29.3	0.588	17.214
C-18	123	576	0	0	28.6	0.392	11.203
C-19	69	591	0.152	89.705	26.2	0.562	14.714
C-20	107	493	0	0	30.6	0.352	10.756
C-21	97	493	0.131	64.563	27.3	0.381	10.403

6. Computer Software-FIN-EC Methods

The fire resistance of reinforced concrete cross-sections is also calculated by structural design software (FIN-EC). [21]. The software uses the finite element method to generate a 3D interaction diagram for the given fire resistance and fire exposure details. The software follows EN 1992-1-2 [14] for analysis results. The results obtained from the software can also be shown in terms of interaction diagram as provided in Figure 12. The interaction diagram displays the defined loads as points. If the load falls within the solid line of the diagram, it means the cross-section meets the fire assessment requirements. On the other hand, the dashed line on the diagram indicates the iteration of the column without buckling. The 500°C Isotherm Method and Zone Method are used in this software to determine the fire resistance of studied columns *(case studies 1 to 3)* and to compare the results obtained from proposed interaction charts. The results obtained from both methods are depicted in Tables 7 and 8.

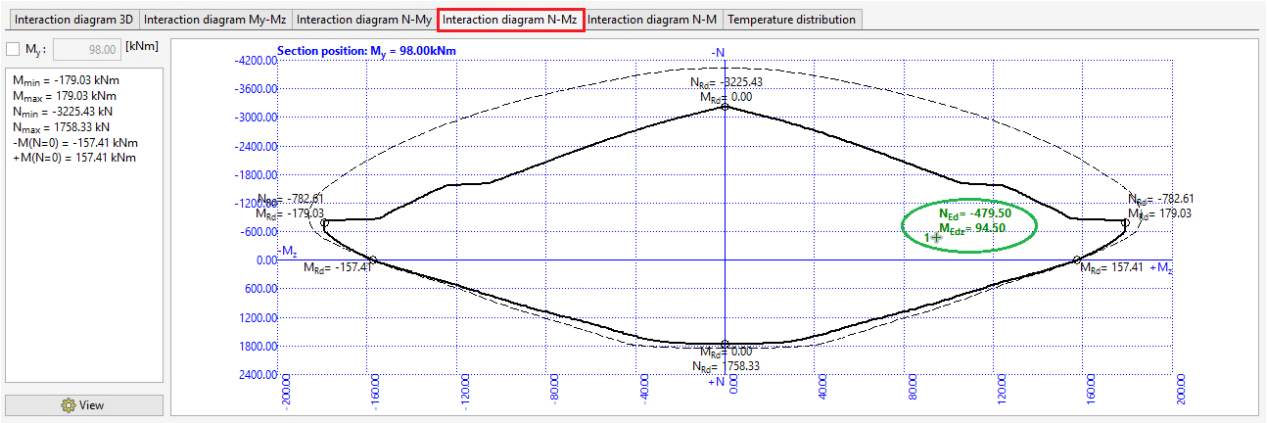

Figure 12. The (*N – Mz)* interaction diagram

Table 7. Column design results of case studies 1 and 2 using Interaction Charts and FIN-EC software

Column Identifier	Steel ratio (ρ)	Gamma (γ)	β Value	α Value	Column Interaction Charts P_N (kN)	FIN-EC (Finite Element Software)	
						500 ºC Method P_N (kN)	Zone Method P_N (kN)
C-1	0.022	0.685	0.620	6.328	583.67	662	841.7
C-2	0.022	0.685	0.474	4.754	442.28	331.5	616.2
C-3	0.022	0.685	0.482	4.855	451.08	324	615.7
C-4	0.022	0.685	0.520	5.223	485.18	505	929.8
C-5	0.022	0.685	0.605	6.049	562.71	1169	1078
C-6	0.022	0.685	0.638	6.518	606.32	666.6	1128.6
C-7	0.022	0.685	0.505	5.089	473.43	485	905.5
C-8	0.022	0.685	0.712	7.120	662.38	453.7	1200
C-9	0.022	0.685	0.648	6.496	604.24	318.7	865
C-10	0.044	0.685	0.602	5.00	465.12	121	605
C-11	0.25	0.764	0.528	7.076	1166	2274	2274
C-12	0.04	0.764	0.863	9.196	1516	2463	2712
C-13	0.022	0.685	0.505	5.067	471.35	180	381
C-14	0.022	0.685	0.537	5.424	504.57	259	408
C-15	0.022	0.685	0.551	6.741	627.09	248	273
C-16	0.022	0.685	0.606	6.071	564.792	415.5	528

Table 8. Column design results of case study 3 using Interaction Charts and FIN-EC software

Column Identifier	Steel ratio (ρ)	Gamma (γ)	β Value	α Value	Column Interaction Chart P_N (kN)	FIN-EC (Finite Element Software)	
						500 °C Method P_N (kN)	Zone Method P_N (kN)
C-17	0.01	0.83	1.026	10.28	925.11	1283	1283
C-18	0.01	0.83	0.612	6.116	550.45	463	508
C-19	0.022	0.83	0.873	9.553	859.82	674	680
C-20	0.01	0.83	0.582	5.848	350.89	397	520
C-21	0.01	0.83	0.620	6.116	367.14	451	543

6.1. 500°C Isotherm Method

In 1978, Andenberg [20] developed the 500°C isotherm method. A version of this method was later published in Eurocode 1992-1-2 [14] and CEB-FIP Bulletin [28]. According to the 500°C isotherm method, if the concrete temperature ranges from 20°C to 500°C, there is no relative reduction in its compressive strength (f_c'). When the temperature exceeds 500°C, the compressive strength (f_c') rapidly deteriorates, remaining at 30% of its initial value when reaching the fire temperature of 700°C. In order to reduce the cross-sectional dimensions of beams or columns due to fire effects, it was assumed that the location of the 500°C isotherm would determine the thickness a_z of the beams or columns. Figure 13 from Krzysztof & Serega [29] shows a reduced cross-section of reinforced concrete beams or columns in the 500°C isotherm method. In the new proposed cross section for normal temperature, concrete properties are similar. It has been shown that yielding stresses in reinforcing steel rebar decrease with temperature level at the middle of each bar, regardless of their location with respect to the 500°C isotherm.

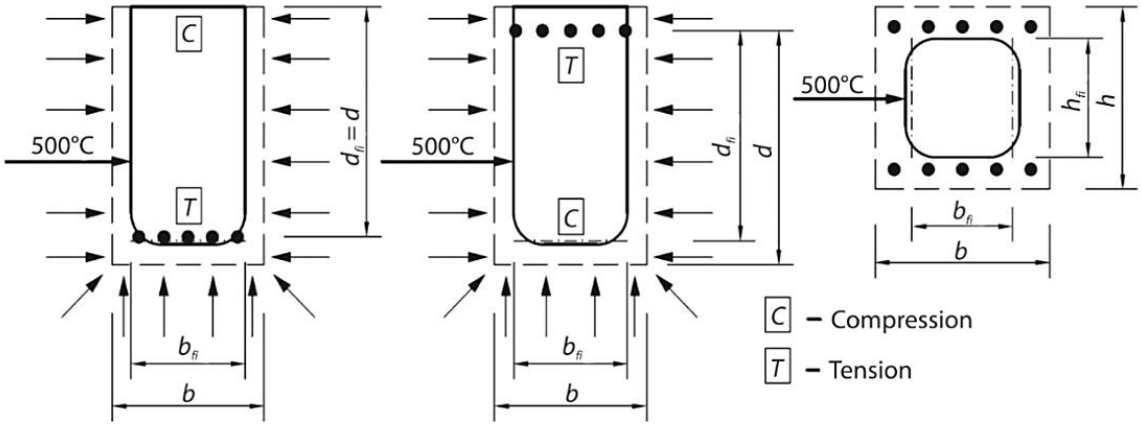

Figure 13. Reduced cross-section of reinforced concrete beam or column in 500°C isotherm method [29]

There are several advantages of the 500°C isotherm method, including that it can be implemented for all cross-section shapes (beams, walls, columns) and that it can be utilized for a variety of heating scenarios (fire from one side, i.e., one face heating, or all four sides, i.e., four face heating). However, this method comes with some limitations.

6.2. Zone Method

An alternative to the 500°C isotherm method was introduced in the eighteenth century by (Hertz [30]) and is known as the zone method. This method was endorsed by Euro-code 2-1-2 [14] for elements subjected to compressive normal force and bending moment.

According to Krzysztof & Serega [29], Figure-14 provides the assumptions and basic notations to calculate the effective cross-section dimensions. In the case of a wall that is heated from both sides, the temperature distribution ($\theta(x)$) can be determined by solving one-dimensional transient heat flow problems. An altered version of the equation for δ_{fc} is provided in Appendix B of Euro-code 2-1-2 [14]. In the case of thin divisions, *n*, the modified form of Equation 30 accounts for significant changes in the temperature range within the zones of each division.

$$a_z = w\left[1-\delta_{fc}\right] \qquad \delta_{fc} = \frac{1-\frac{1}{5n}}{n}\frac{\sum_{i=1}^{n} k_c(\theta_i)}{k_c(\theta_M)} \tag{30}$$

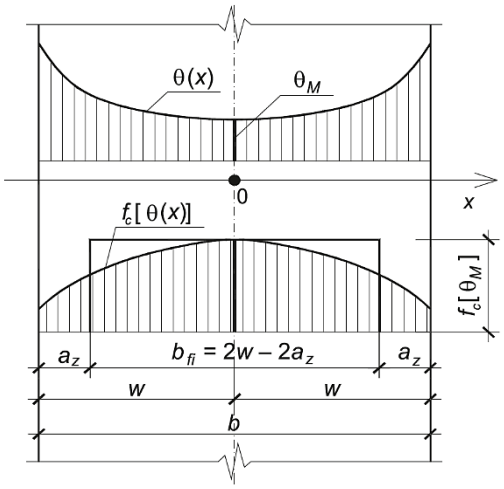

Figure 14. Assumptions and notations for zone method [29]

Euro-code 2-1-2 [14], Appendix B provides comprehensive information on the reduction of cross-sectional dimensions of various shapes by a specific value a_z. The zone method is akin to the 500°C isotherm method, as it employs conventional concrete structural theory to determine fire resistance, $R_{fi}(t)$. Computations are conducted for the diminished geometry of cross-sections, the reduced yielding stress for steel $f_{y-red} = k_s(\theta_s)f_y(20°C)$, (where θs is the temperature of the reinforcing steel), and the reduced compressive strength of concrete obtained using the equation $f_{c-red} = k_c(\theta_M)f_y(20°C)$ [29]. The temperature profiles for square and rectangular column cross-sections (*column C-4 and column C-20*) using the zone method and the 500°C isotherm method in FIN-EC software are depicted in Figures 15 and 16, respectively.

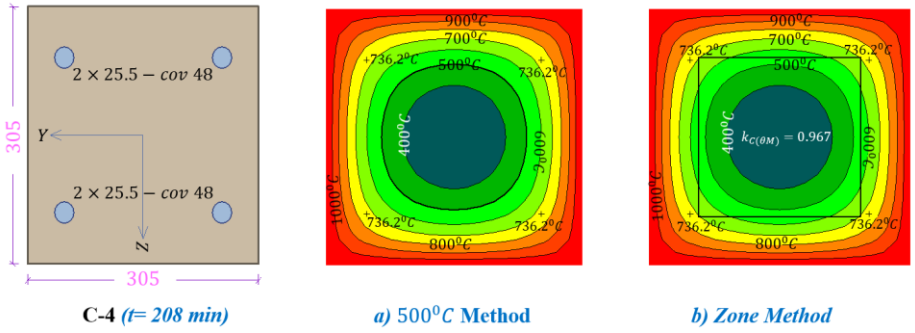

Figure 15. Temperature profile for square column section *(C-4)*

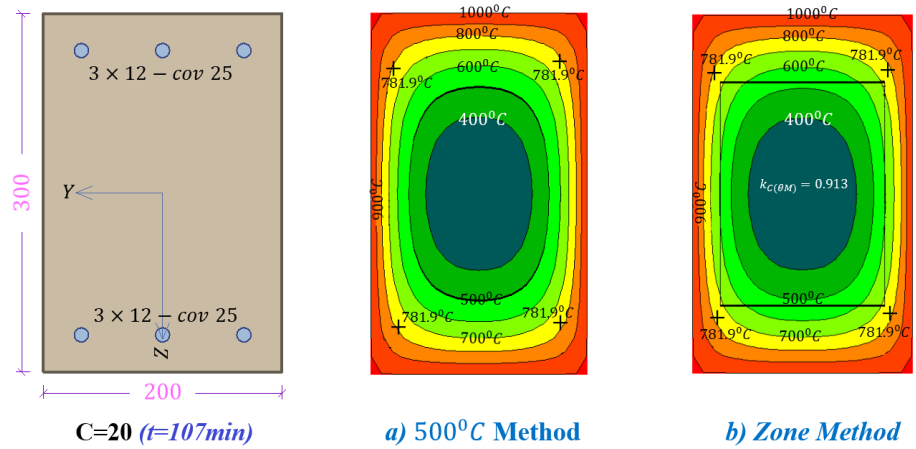

Figure 16. Temperature profile for rectangular column section *(C-20)*

Jaszczak et al. [31] examined the load-bearing capability of reinforced concrete (RC) columns during fire circumstances utilizing three distinct methods: Method A, Zone Method, and Isotherm 500 Method. The Zone Method is the most suitable for accounting for second-order effects, with the smallest standard deviation and an average value

closest to the expected value among the methods tested. However, this method requires determining the temperature distribution in the cross-section. Despite being unrestricted in use, the Isotherm 500 Method is the least accurate. They also emphasized that when selecting a model for structures under fire, simplicity and validity should be the guiding principle.

7. Results and Discussions

The results of case studies 1 to 3 using the proposed uniaxial column interaction charts are provided in Tables 7 and 8. All the required parameter values; steel ratio (ρ), gamma value (γ), alpha (α) and beta (β) values needed in the calculating the axial load value, P_N *(kN)* using the charts are also provided in this table. Moreover, the results obtained using the FIN-EC software are also depicted in these Tables 7 and 8.

The comparison of results is provided in Table 9 for case studies 1 and 2, and in Table 10 for case study-3. The results showed a safe and conservative proposed column interaction chart. Figure 17 shows the scatter plot for the axial load of studied columns using the proposed charts verses the values obtained from studied cases and computer software. Generally, the proposed interaction charts showed a good correlation with the experimental results provided in all three case studies having the coefficient of determination (R^2) value ≥ 80.1%. The R^2 value can be calculated from the following Equation 30.

$$R^2 = 1 - \frac{\sum_{i=1}^{N}(y_i - \hat{y}_i)^2}{\sum_{i=1}^{N}(y_i - \bar{y})^2} \quad (30)$$

where; y represents the target values, ŷ denotes the predicted values, ȳ signifies the mean of the y values, and N refers to the number of tested columns for each case study.

Table 9. Comparison results of case studies 1 and 2

Column Identifier	Column Interaction Chart $P_{N(C-I)}$(kN)	FIN (Finite Element Software)		Lie & Woollerton (1988) Axial Load $P_{N(L-W)}$ (kN)	Bo Wu et.al (2007) Axial Load $P_{N(BO)}$ (kN)	$\frac{P_{N(C-I)}}{P_{N(L-W)}}$	$\frac{P_{N(C-I)}}{P_{N(BO)}}$
		500 ºC Method P_N (kN)	Zone Method P_N (kN)				
C-1	583.67	662	841.7	1333	517.2	0.437	1.12
C-2	442.28	331.5	616.2	800	200	0.552	2.21
C-3	451.08	324	615.7	711	155	0.634	2.91
C-4	485.18	505	929.8	1067	339	0.454	1.43
C-5	562.71	1169	1078	1333	498.5	0.422	1.12
C-6	606.32	666.6	1128.6	1044	268	0.580	2.26
C-7	473.43	485	905.5	916	255	0.516	1.85
C-8	662.38	453.7	1200	1178	280	0.562	2.36
C-9	604.24	318.7	865	1067	247.5	0.566	2.44
C-10	465.12	121	605	978	242	0.475	1.92
C-11	1166	2274	2274	2418	914	0.482	1.27
C-12	1516	2463	2712	2978	NA	0.509	NA
C-13	471.35	180	381	800	NA	0.589	NA
C-14	504.57	259	408	1000	NA	0.504	NA
C-15	627.09	248	273	1000	NA	0.627	NA
C-16	564.792	415.5	528	1178	NA	0.479	NA

Table 10. Comparison results of case study-3

Column Identifier	Column Interaction Chart $P_{N(C-I)}$ (kN)	FIN (Finite Element Software)		Dotreppe et al. (1997) Axial Load $P_{N(D)}$ (kN)	$\frac{P_{N(C-I)}}{P_{N(D)}}$
		500 ºC Method P_N (kN)	Zone Method P_N (kN)		
C-17	925.11	1283	1283	1270	0.728
C-18	550.45	463	508	803	0.685
C-19	859.82	674	680	878	0.979
C-20	350.89	397	520	611	0.574
C-21	367.14	451	543	620	0.592

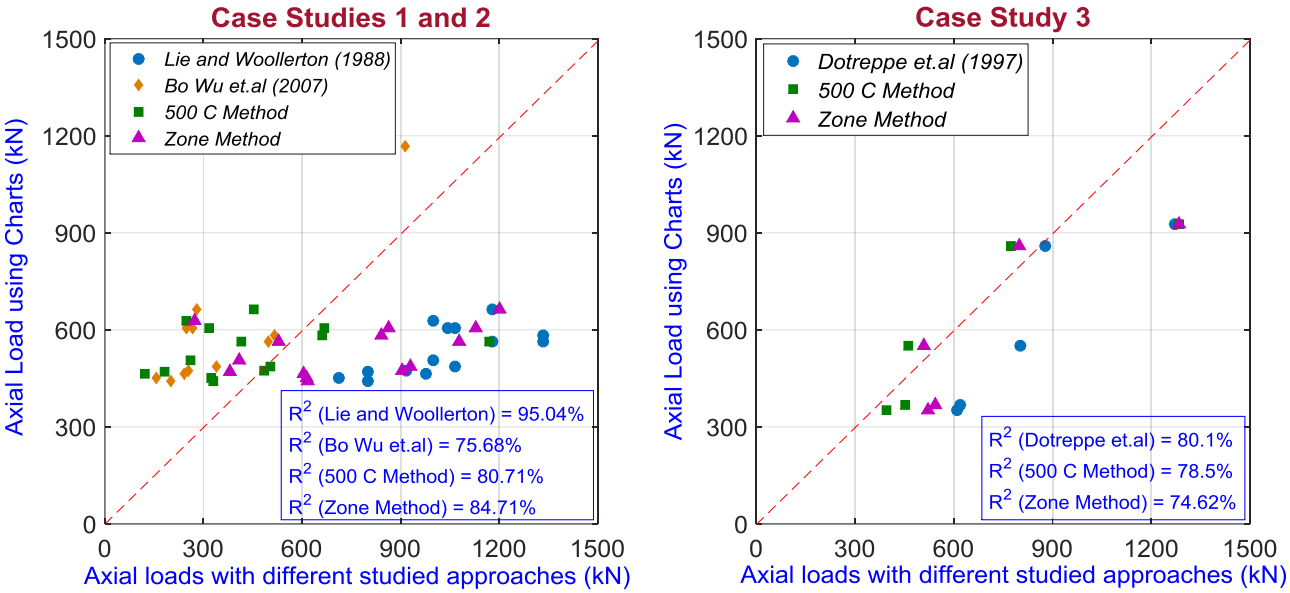

Figure 17. Comparison of axial load for all case studies

The current study proposes interaction charts for determining the axial load capacity of uniaxial columns under four face heating. The values obtained using these charts are relatively close to the experimental values in both case studies 1-2 and 3, indicating a simple and quick method for determining axial load capacity. The values provided by (Lie & Woollerton [8]) and (Wu, et al. [17]) differ because they used different approaches to find the axial load capacities (Figure 18). However, In the two case-studies *(case study 1 and 2)*, the zone method produced relatively good results that were also conservative when compared to the 500 ^{0}C method. This suggests that the zone method approach used in the computer software is a more reliable for evaluating the load-bearing capacity of reinforced concrete columns exposed to fire. In case study 3, which examines columns C-17 to C-21 and refers to the work of Dotreppe et al. [7], the bar chart in Figure 19 shows that the proposed interaction charts provide results that are much closer to the experimental values. Furthermore, the results are consistent with those obtained from the zone and 500 ^{0}C methods.

The results obtained from case studies 1 and 2 where the fire time was more than 2.5 hours were between the laboratory results and computer software outputs. The proposed interaction charts showed a coefficient of determination ranging from 75% to 95%. This also indicated that the zone method performs well in situations where the fire duration is long. For case study 3 where the fire time was less than 125 minutes, the results obtained using 500 ^{0}C method were also close to zone method. This suggests that in scenarios with less fire time, the 500 ^{0}C method can also be effective in predicting the axial load capacities of reinforced concrete columns.

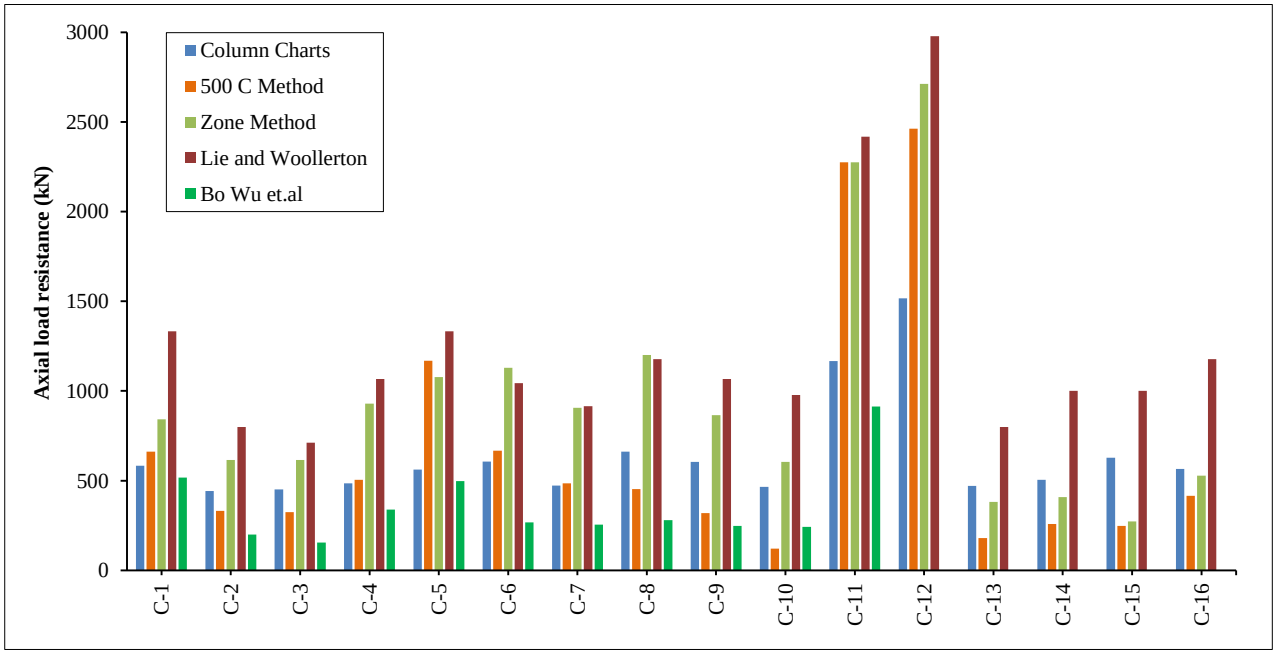

Figure 18. Axial load comparison for case studies 1 and 2

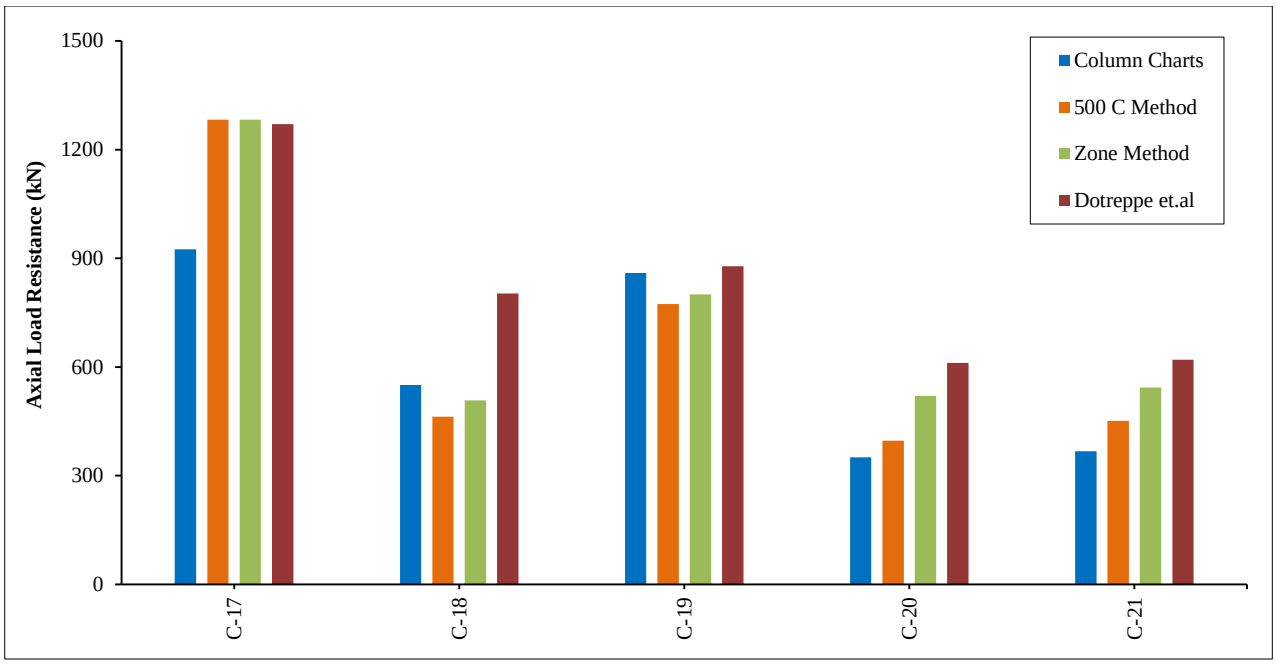

Figure 19. Axial load comparison for case study-3

The proposed method's values fall within the range of values obtained from laboratory tests and computer software, which suggests its validity. These findings indicates that the proposed interaction charts are a reliable and accurate method for determining the axial load capacity of reinforced concrete columns exposed to fire. The study's findings have implications for the field of structural engineering, as they offer a simple and quick method for determining the axial load capacity of uniaxial columns under four face heating. This can be useful in designing and analysing structures exposed to fire. The strength of the study lies in proposing a simple and quick method for determining axial load capacity. However, the study only focuses on uniaxial columns under four face heating, limiting its applicability to other types of structures and heating conditions.

8. Conclusion

The study presents an analytical method for generating interaction diagrams of uniaxial reinforced concrete columns under fire conditions exposed to four face heating. The study proposes the use of reduction factors ϕ_{c-4} and ϕ_{y-4}, *(for concrete and steel bars respectively for four face heating)*, for calculating reduced compressive strength and reduced steel yield strength, based on the SAFIR model under ISO 834 fire, in a study conducted by (Tan & Yao, [5]). The proposed interaction charts provide reliable results for determining the axial load capacity of reinforced concrete columns exposed to fire. The zone method used in FIN-EC software is a more reliable approach than the 500°C method, and the load values obtained from the proposed charts fall between the laboratory test results and computer software outputs.

The study contributes to new knowledge by proposing a simple and quick method for determining axial load capacity in uniaxially reinforced concrete columns exposed to four-face heating. The study's proposed interaction charts are a reliable and accurate tool for structural engineers designing and analyzing structures exposed to fire. The study's focus on the SAFIR model's reduction factors offers a valuable contribution to the field. During a fire outbreak in a reinforced concrete building, the concrete and steel rebar strength will significantly decrease. Therefore, reduction factors are essential when determining the new design strengths of reinforced concrete columns. Conducting experiments on reinforced concrete columns under fire conditions is costly and challenging, and the laboratory setups differ from real-life scenarios of fire outbreaks. In addition, the experimental results provide an approximate prediction of the reduced compressive strength of reinforced concrete columns, which comes at a cost. Due to the difficulty of preparing laboratory fire chambers, researchers use available analytical approaches to predict values that are relatively close to experimental results.

The study is limited in its focus on only uniaxial columns under four-face heating, which restricts its applicability to different types of structures and heating conditions. Future research should examine other boundary conditions and factor in imperfections to determine the load-bearing capacity of reinforced concrete columns under fire conditions. Doing so will provide more reliable models for engineers to design and analyze structures that may be exposed to fire.

9. Declarations

9.1. Author Contributions

Conceptualization, M.S.Al.; methodology, M.S.Al.; software, M.S.Al.; validation, M.S.Al. and M.S.A.; formal analysis, M.S.Al.; investigation, M.S.Al. and M.S.A.; resources, M.S.Al. and M.S.A.; data curation, M.S.Al. and M.S.A.; writing—original draft preparation, M.S.A.; writing—review and editing, M.S.Al. and M.S.A.; visualization, M.S.Al. and M.S.A.; supervision, M.S.Al.; project administration, M.S.Al. and M.S.A.; funding acquisition, M.S.Al. All authors have read and agreed to the published version of the manuscript.

9.2. Data Availability Statement

The data used to support the findings of this study are available from the corresponding author upon request.

9.3. Funding

The publication of this article was funded by Qatar National Library, Doha, Qatar.

9.4. Conflicts of Interest

The authors declare no conflict of interest.

10. References

[1] Anderberg, Y. (1983). Predicted fire behaviour of steels and concrete structures. LUTVDG/TVBB--3011--SE; Volume 3011, Division of Building Fire Safety and Technology, Lund Institute of Technology, Lund, Sweden.

[2] Burgess, I. W., & Najjar, S. R. (1994). A simple approach to the behaviour of steel columns in fire. Journal of Constructional Steel Research, 31(1), 115–134. doi:10.1016/0143-974X(94)90027-2.

[3] Kodur, V. K. R., Wang, T. C., & Cheng, F. P. (2004). Predicting the fire resistance behaviour of high strength concrete columns. Cement and Concrete Composites, 26(2), 141–153. doi:10.1016/S0958-9465(03)00089-1.

[4] Al-Ansari, M. S., & Afzal, M. S. (2020). Mathematical model for analysis of uniaxial and biaxial reinforced concrete columns. Advances in Civil Engineering, 8868481. doi:10.1155/2020/8868481.

[5] Tan, K. H., & Yao, Y. (2003). Fire resistance of four-face heated reinforced concrete columns. Journal of Structural Engineering, 129(9), 1220-1229. doi:10.1061/(ASCE)0733-9445(2003)129:9(1220).

[6] Dotreppe, J. C., Franssen, J. M., & Vanderzeypen, Y. (1999). Calculation method for design of reinforced concrete columns under fire conditions. ACI Structural Journal, 96(1), 9–18. doi:10.14359/591.

[7] Dotreppe, J. C., Franssen, J. M., Bruls, A., Baus, R., Vandevelde, P., Minne, R., Van Nieuwenburg, D., & Lambotte, H. (1997). Experimental research on the determination of the main parameters affecting the behaviour of reinforced concrete columns under fire conditions. Magazine of Concrete Research, 48(6), 117–127. doi:10.1680/macr.1997.49.179.117.

[8] Lie, T. T., & Woollerton, J. L. (1988). Fire resistance of reinforced concrete columns: test results. National Research Council Canada, Institute for Research in Construction, Quebec, Canada.

[9] Zhou, X., Yang, J., Liu, J., Wang, S., & Wang, W. (2021). Fire resistance of thin-walled steel tube confined reinforced concrete middle-length columns: Test and numerical simulation. Structures, 34, 339–355. doi:10.1016/j.istruc.2021.07.078.

[10] Martins, A. M. B., & Rodrigues, J. P. C. (2010). Fire resistance of reinforced concrete columns with elastically restrained thermal elongation. Engineering Structures, 32(10), 3330–3337. doi:10.1016/j.engstruct.2010.07.005.

[11] Xu, Y., & Wu, B. (2009). Fire resistance of reinforced concrete columns with L-, T-, and +-shaped cross-sections. Fire Safety Journal, 44(6), 869–880. doi:10.1016/j.firesaf.2009.04.002.

[12] Kodur, V., & McGrath, R. (2003). Fire endurance of high strength concrete columns. Fire Technology, 39(1), 73–87. doi:10.1023/A:1021731327822.

[13] Franssen, J. M., & Dotreppe, J. C. (2003). Fire tests and calculation methods for circular concrete columns. Fire Technology, 39(1), 89–97. doi:10.1023/A:1021783311892.

[14] ENV 1992-1-2:2004. (2004). Eurocode 2: Design of concrete structures – Part 1.2: General rules Structural fire design, European Committee for Standardization, Brussels, Belgium. doi:10.3403/03213853u.

[15] Phan, L. T., & Carino, N. J. (1998). Review of Mechanical Properties of HSC at Elevated Temperature. Journal of Materials in Civil Engineering, 10(1), 58–65. doi:10.1061/(asce)0899-1561(1998)10:1(58).

[16] Kodur, V., & McGrath, R. (2001). Performance of high strength concrete columns under severe fire conditions. CONSEC'01: Third International Conference on Concrete Under Severe Conditions, 18-20 June, 2001, Vancouver, Canada.

[17] Wu, B., Hong, Z., Tang, G. H., & Wang, C. (2007). Fire resistance of reinforced concrete columns with square cross section. Advances in Structural Engineering, 10(4), 353–369. doi:10.1260/136943307783239336.

[18] Kang, H., Cheon, N. R., Lee, D. H., Lee, J., Kim, K. S., & Kim, H. Y. (2017). P-M interaction curve for reinforced concrete columns exposed to elevated temperature. Computers and Concrete, 19(5), 537–544. doi:10.12989/cac.2017.19.5.537.

[19] Tan, K. H., & Yao, Y. (2004). Fire Resistance of Reinforced Concrete Columns Subjected to 1-, 2-, and 3-Face Heating. Journal of Structural Engineering, 130(11), 1820–1828. doi:10.1061/(asce)0733-9445(2004)130:11(1820).

[20] Andenberg, Y. (1978). Analytical fire design of reinforced concrete structures based on real fire characteristics. FIB Eight Congress Proceedings, 1(30), April-5 May, 1978, London, United Kingdom.

[21] FIN EC Structural Software (2023). Intuitive suite for frames, individual elements and details. Prague, Czech Republic. Available online: https://www.finesoftware.eu/structural-analyses/ (accessed on April 2023).

[22] ISO-834-13. (2019). Fire-resistance tests-Elements of building construction-Part 13: Requirements for the testing and assessment of applied fire protection to steel beams with web openings. International Organization for Standardization (ISO), Geneva, Switzerland.

[23] Franssen, J.M., (1999). Manual of SAFIR. Civil and Structural Engineering Department, University of Liege, Liège, Belgium.

[24] Al-Ansari, M. S., & Afzal, M. S. (2019). Simplified biaxial column interaction charts. Engineering Reports, 1(5), 1-15. doi:10.1002/eng2.12076.

[25] Rodrigues, H., Romão, X., Andrade-Campos, A., Varum, H., Arêde, A., & Costa, A. G. (2012). Simplified hysteretic model for the representation of the biaxial bending response of RC columns. Engineering Structures, 44, 146-158. doi:10.1016/j.engstruct.2012.05.050.

[26] ACI 318-19. (2019). Building Code Requirements for Structural Concrete and Commentary. American Concrete Institute (ACI), Michigan, United States. doi:10.14359/51716937.

[27] James, G., MacGregor, J. G., & Wight, J. K. (2015). Reinforced Concrete: Mechanics and Design (8th Ed.). Prentice Hall, Hoboken, United States.

[28] fib CEB-FIP. (1991). Fire Design of Concrete Structures in Accordance with CEB-FIP Model Code 90-Final Draft. Bulletin d'Information du CEB, (208), Lausanne, Switzerland.

[29] Chudyba, K., & Seręga, S. (2013). Structural fire design methods for reinforced concrete members. Czasopismo Techniczne, Technical Transactions, Civil Engineering, 1-B/2013.

[30] Hertz, K. D. (2019). Fire exposure. Design of Fire-resistant Concrete Structures. ICE publishing, London, United Kingdom. doi:10.1680/dofrcs.64447.051.

[31] Jaszczak, B., Kuczma, M., & Szymkuć, W. (2021). Comparison of the load-bearing capacity of reinforced concrete columns under fire conditions using the method A, zone method and isotherm 500 method. Fire Safety Journal, 124, 103396. doi:10.1016/j.firesaf.2021.103396.